Determination of the Deactivation Model of Iron-potassium/γ-Al₂O₃ Catalyst in a Fixed Bed Reactor

H. Atashi* and S. Veiskarami

University of Sistan and Baluchestan, Department of Chemical Engineering

(Received 14 January 2018, Accepted 26 March 2018)

Catalyst activity and performance are the most important factors for selecting a catalyst in different processes. The Fischer-Tropsch synthesis is a very important synthesis that extensive action has been taken place to increase the activity of its catalysts (mainly cobalt and iron) in the recent century. Deactivation of the catalysts of the process is influenced by many factors, among which coking and sintering have come to be considered as key causes of the catalysts deactivation over time. Determination of the deactivation model for catalysts based on empirical data causes the catalyst activity and efficiency to be predictable, which, in turn, can significantly reduce the cost of construction and processing at industrial scale up. An Fe-K/Al₂O₃ catalyst was prepared by using an impregnation method in this research. Experimental data were measured in a fixed-bed tube reactor under low operating pressure (0.2 MPa) and high temperature (310 °C). By comparing the experimental data (in this study) with different models of deactivation, was obtained as the best model for the deactivation of Fe-K/Al₂O₃ catalyst that amounts of k_d, a_{eq} and m are 0.425, 0.459 and 1, respectively. Then, the experimental data obtained from this study were compared with those of the other references to evaluate the effectiveness of potassium promoter and alumina support on the parameters of the deactivation rate equation (as k_d, a_{eq} and m). It was found that alumina support at high operating pressures and low temperatures can reduce the deactivation rate of iron-based catalyst in the presence of K promoter.

Keyword: Fischer-Tropsch synthesis, Fe-K/Al₂O₃ catalyst, Fixed bed reactor, Equation of deactivation rate

INTRODUCTION

Many industrial processes are possible just in the presence of catalysts. All attempts are being made to increase the catalyst activity and stability in these industrial processes. Decline of the catalyst activity and, after then, the cessation of the process and again reduction of the catalyst have a heavy cost. For this purpose, huge costs are paid for the more utilization and control of process for the late deactivation of catalysts. Included in the catalytic processes is noted Fischer-Tropsch (FT) process. The FT process is a strongly exothermic catalytic process that produces oil derivatives free of sulphur from synthesis gases derived from carbon sources such as coal, biomass and natural gas during numerous reactions [1-7]. The most

catalysts used in this synthesis are based on cobalt and iron [8,9]. These two metals, in addition to stability and appropriate activity, are the most economical catalysts compared to other metals [10,11]. The most important issue in catalysts is the decline in catalyst activity over time, and this phenomenon is called the deactivation of catalysts. It occurs due to changes in the chemical nature or physical structure. Factors such as reaction temperature, catalyst structure, and reaction products can have a significant role in the rate of the catalyst deactivation, making it difficult to identify the source of the deactivation [12,13]. Generally, the reduced activity of catalysts could be due to four reasons: 1) oxidation of the active phases to the passive phases; 2) deposition of carbon components; 3) sintering; and 4) poisoning by impurities such as sulphur in the input feed material [14-16]. Promoter and support are used to decrease the rate of catalyst deactivation. Among these, the

_____
*Corresponding author. E-mail: H.ateshy@hamoon.usb.ac.ir

potassium promoter and alumina support for iron-based catalyst are notable. Potassium is considered an electron promoter for the iron-based catalysts [17,18]. This metal, due to its strong basic structure, increases the sustainability of iron-based catalysts, and, by absorbing reactants in active sites, increases the percentage of CO conversion, thus plays the role of a catalyst [19]. The alumina support also causes the distribution of iron particles on its surface by creating groups of Al-OH and, with this performance, in addition to increase the surface area, prevents early sintering and agglomeration of catalyst [20]. Ki-Won Jun *et al*. examined the support effect on the iron and the iron-potassium catalyst. They found the strong interaction for iron on the TiO_2 support and a lower CO conversion percentage on the alumina support. However, when the potassium is added to the Fe/Al_2O_3 catalyst, further CO conversion rate is expected [21]. Cubeiro prepared the $Fe-K/Al_2O_3$ catalyst in three methods of impregnation, deposition and physical mixing to study the products of CO and CO_2 under the Fischer-Tropsch synthesis. He concluded that the carbon dioxide feed has a more production of the long-chain hydrocarbons than CO [22]. Sun-Jin Choung studied binders such as silica, alumina, and PVA in the $Fe-K/Al_2O_3$ catalyst. His results indicated that the alumina binder increases the selectivity of heavy hydrocarbons due to the increase in catalyst acid sites [23].

The rate of catalyst deactivation and its reasons should be considered in the design of the industrial equipment. For example, the deactivation of catalysts in the presence of carbon components in critical conditions causes the collapse of the catalyst and closure of the reactor output currents, and/or a sharp decline in production as the result of the deactivation of the catalyst by sintering [12]. The process of change in the catalyst activity can be obtained by using deactivation equations over time and it can be used in the design of equipment. Despite the high importance of the deactivation phenomenon in catalytic processes, few projects have been done on the deactivation of catalysts. In 1991 and 1999, C. H. Bartholomew examined the rate of deactivation of iron-potassium and iron catalysts on the monolith at low and high pressures, respectively [24,25]. Ji-Sook Hong reviewed the deactivation of Fe-Cu-K-Al catalyst and expressed the increase of iron phase crystals as the main reason for its deactivation, in such a way that, the

growth of crystalline phases decreases the activity of Cu, and K promoter [26]. At the same time, Jin Soo Hwang indicated the deactivation of $Fe-K/Al_2O_3$ catalyst due to the increase of carbon on the catalyst active surface [15] but did not offer a comprehensive model for deactivation of this catalyst. In this research, the objective is to provide a comprehensive and thorough model for the deactivation rate of the $Fe-K/Al_2O_3$ catalyst according to the experimental data obtained in this study in a fixed bed tube reactor, and also all parameters of the deactivation rate will be obtained. In catalytic processes, the catalyst performance in the reactor causes a change in the output pressure as well as the amount of products; and therefore, has a direct effect on the design of the equipment out of the reactor. The performance of the reactor at different times can be predicted with deactivating models. We also identified the factors affecting the loss of catalyst activity and sought to cope with them.

EXPERIMENT

Catalyst Production

An industrial alumina was used as support in this research. Before making the catalysts, in order to clean the supports, they were calcinated at 500 °C for 5 h. In doing so, the catalyst was made by the impregnation method. The amount of 9.8 g of $Fe(NO_3)_3.6H_2O$ and 0.96 g of potassium nitrate were dissolved in 30 cc and 5 cc of the sterile water, respectively. Both solutions were poured on the supports simultaneously and the obtained mixture was kept in the fresh air for 30 min. As soon as the supports were separated from the solution, they were placed in the open air for 20 minutes to reduce their moisture content. The drying operation under 200 °C lasted for 4 h. Calcination was also done at the speed of 5 °C min^{-1} and temperature of 500 °C, through which 44 g of the $Fe-K/Al_2O_3$ catalyst was obtained. The method of catalyst making is shown in Fig. 1.

Reactor

As can be seen in Fig. 2, a fixed-bed tube reactor was used in this study. One gram of the $Fe-K/Al_2O_3$ catalyst was placed with suitable distribution (for layer by layer, by using industrial fibreglass) to the most conversion of CO in the reactor. Reduction was done by hydrogen gas under the incoming flow of 15 ml min^{-1} and at a temperature of
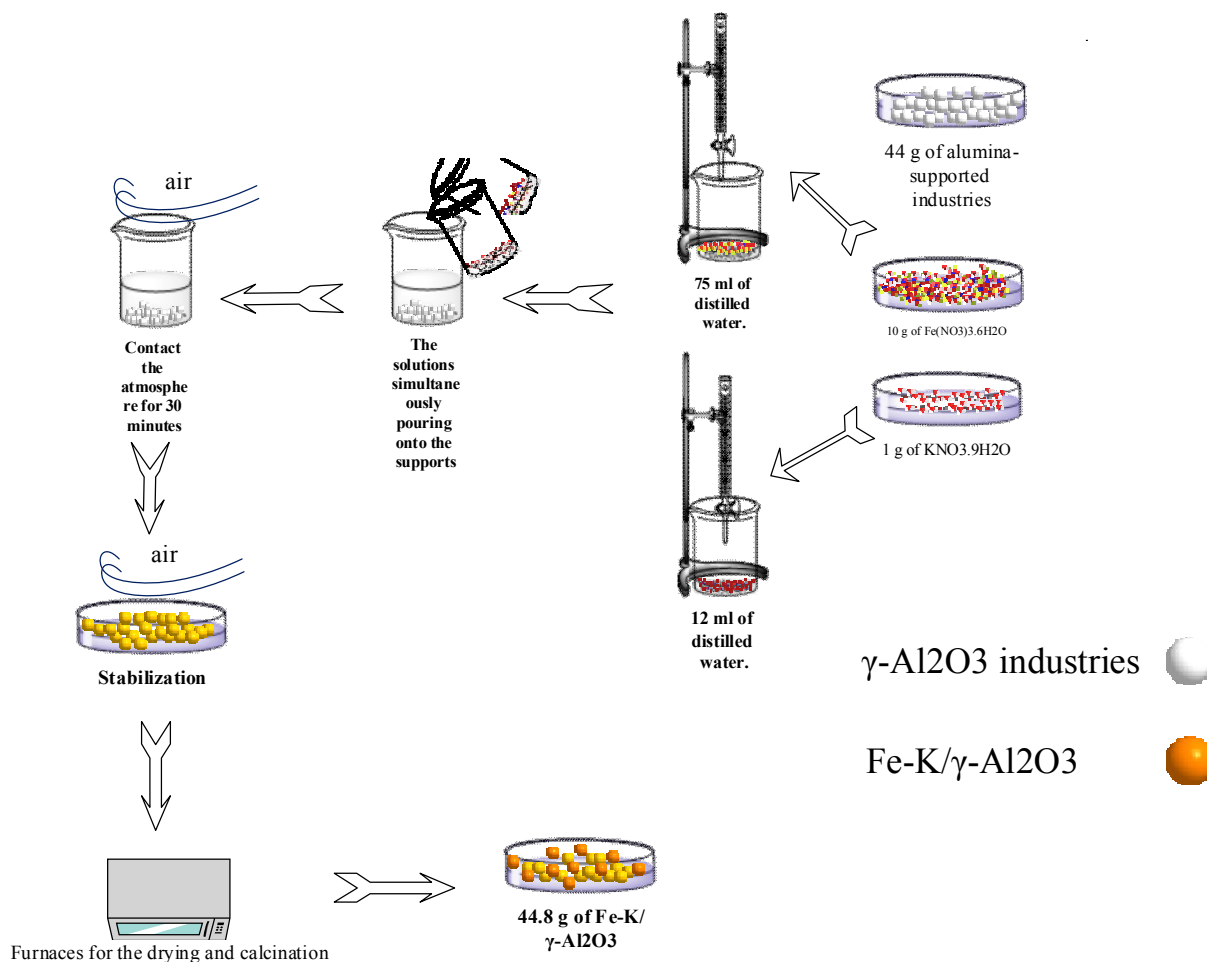
Fig. 1. Production of Fe-K/γ-Al$_2$O$_3$ catalyst by the impregnation method.

500 °C and pressure of 0.2 MPa for 24 h. The use of hydrogen was to increase the thermal stability of the catalyst [27]. Then the catalyst was placed under the operating conditions at T = 310 °C, 0.2 MPa of pressure, and input flow of H$_2$/CO = 1, GHSV = 2400 h^{-1}. Next, gases produced were identified and recorded by the gas chromatography device.

Test Conducting Method

One gram of the catalyst was placed under reaction conditions for 2 h, and the conversion percentage of CO was measured. Then, the catalyst was removed from the reactor to obtain the percentage of CO conversion in the next point, and the new catalyst was placed under the reduction

conditions similar to that of the previous test. The catalyst was under the reaction operation for 4 hours and the next point was determined. The experimental data were obtained in this order. Each test was repeated thrice to increase accuracy, and their average was calculated.

Achieving the Optimal Conversion

Before doing the main tests, the optimum operating condition was achieved for the most conversion of CO in the Fe-K/γ-Al$_2$O$_3$ catalyst. To do so, the necessary changes in the temperature, the gas flow rate and time of the catalyst reduction were applied. A summary of actions taken to achieve optimal operating conditions is included in Table 1. Finally, the third operating conditions were accepted.
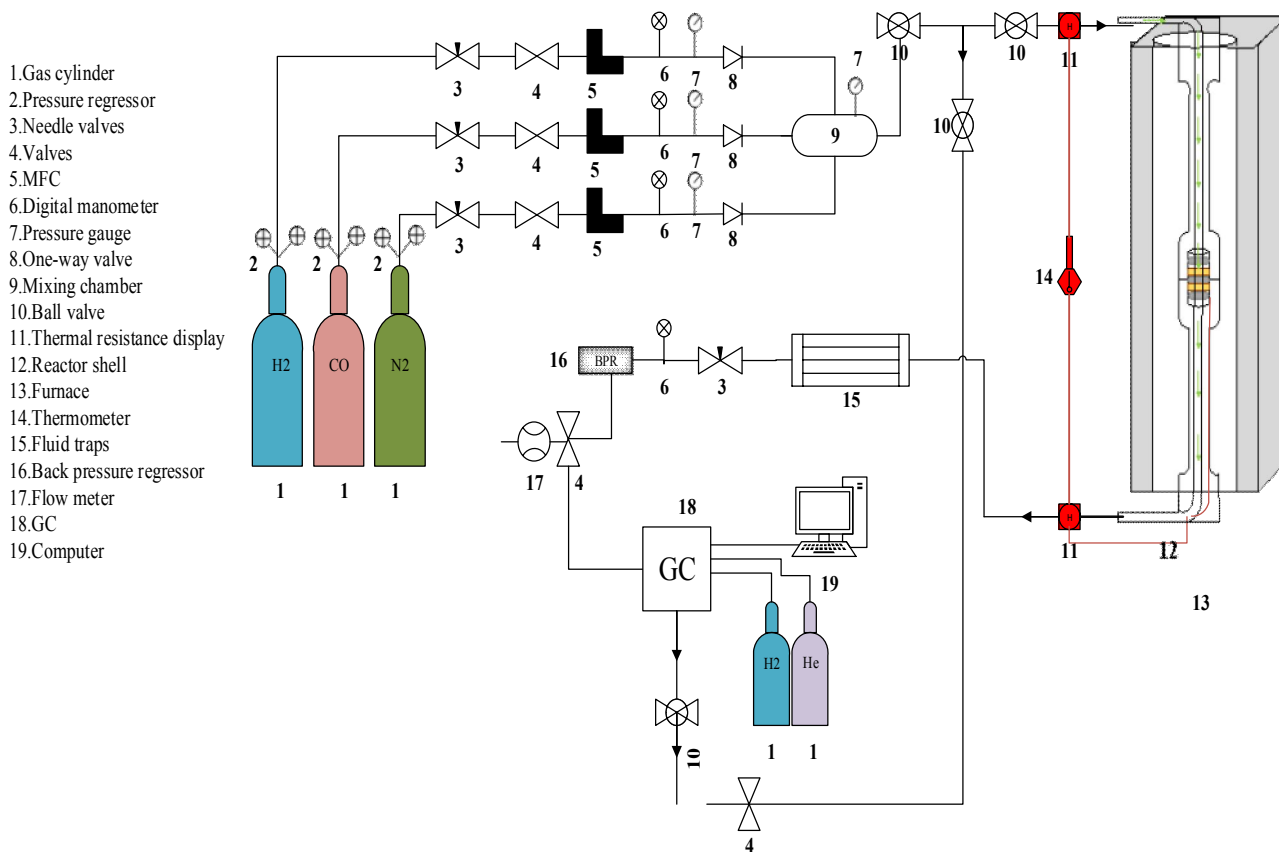
367

1.Gas cylinder
2.Pressure regressor
3.Needle valves
4.Valves
5.MFC
6.Digital manometer
7.Pressure gauge
8.One-way valve
9.Mixing chamber
10.Ball valve
11.Thermal resistance display
12.Reactor shell
13.Furnace
14.Thermometer
15.Fluid traps
16.Back pressure regressor
17.Flow meter
18.GC
19.Computer

Fig. 2. A schematic of fixed-bed tube reactor used in this study.

METHODOLOGY

Different forms can explain the rate of decline in catalytic activity over time. The experimental equations of the
rate of deactivation are as follows:

$$r_{dP} = -\frac{da}{dt} = k_d a_P^z \qquad (1)$$

$$r_{dG} = -\frac{da}{dt} = k_d'\left(a_G - a_{eq}\right)^m \qquad (2)$$

In the Eqs. (1) and (2), a is the normalized activity and is equal to the rate of reaction at any time per the initial rate of the reaction. a_{eq} is normal activity at infinite time, and k_d and k_d' represent the deactivation rate constant without and

with a_{eq}, respectively. Moreover, r_{dP} and r_{dG} represent the rate of catalyst deactivation without and with a_{eq}, respectively. z is the degree of deactivation for r_{dP} and m is the degree of deactivation for r_{dG}.

If the deactivation degrees are considered 1 and 2, by the integration of the Eqs. (1) and (2), the normalized activity will be:

$$a_{P1} = \exp(-k_d t) \qquad z = 1 \qquad (3)$$

$$a_{p2} = \frac{1}{1 - k_d t} \qquad z = 2 \qquad (4)$$

$$a_{G1} = a_{eq} + (1 - a_{eq}) \times \exp(-k_d'.t) \qquad m = 1 \qquad (5)$$

Table 1. Determination of the Optimum Operating Condition

Test	Temperature (°C)	Pressure (Bar)	Flow H$_2$ (ml min^{-1})	Flow CO (ml min^{-1})	Time (h)	%Conversion of CO
Reduction Condition (1)	400	2	30	-	24	-
Operation Condition (1)						
1	280	2	30	30	2	1.8
2	300	2	30	30	2	2.15
3	320	2	30	30	2	3.2
4	350	2	30	30	2	3.9
5	370	2	30	30	2	6.3
Reduction Condition (2)	450 + 500	2	15	-	6 + 30	-
Operation Condition (2)						
1	420	2	20	20	2	69.5
2	400	2	20	20	2	40.2
3	380	2	20	20	2	25
Reduction Condition (3)	500	2	15	-	24	-
Operation Condition (3)						
1	310	2	20	20	2	84.1

$$a_{G2} = a_{eq} + \left((k_d'.t) + \frac{1}{1 - a_{eq}} \right)^{-1} \qquad (6)$$

The best equation can be obtained for the deactivation rate of Fe-K/Al$_2$O$_3$ catalyst by matching the Eqs. (3)-(6) with experimental data obtained in this study.

RESULTS AND DISCUSSION

Determination of the Equation of Deactivation Rate of the Fe-K/Al$_2$O$_3$ Catalyst

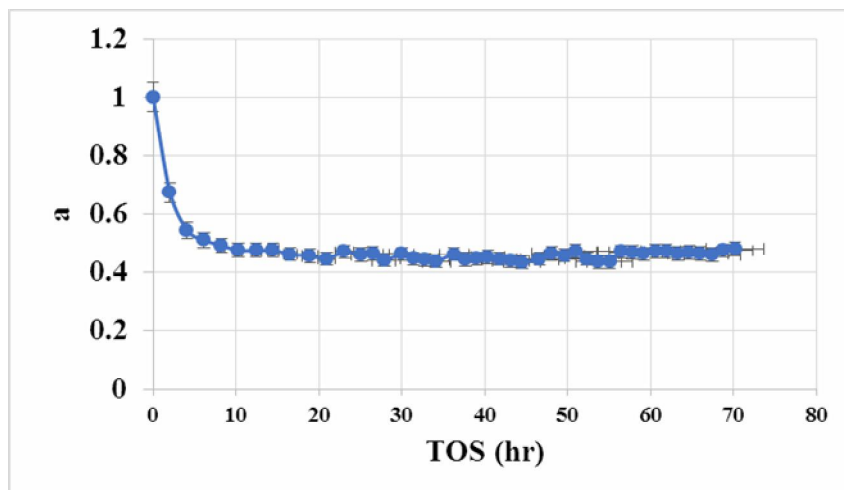The conversion of CO for the Fe-K/Al$_2$O$_3$ catalyst was

Fig. 3. Change of activity over time in the FTS on the Fe-K/γ-Al$_2$O$_3$ catalyst in a fixed bed reactor.

obtained with Eq. (7):

$$X_{CO} = \frac{C_{CO_{in}} - C_{CO_{out}}}{C_{CO_{in}}} \tag{7}$$

The normal activity is obtained with the Eq. (8) and it can be seen in Fig. 3.

$$a = \frac{X_{CO}}{X_{CO,max}} \tag{8}$$

$X_{CO,max}$ is the maximum of CO conversion.

In Fig. 3, it is obvious that the activity of the catalyst has been decreased to 70 % and 65.4% in 24 h and 72 h, respectively. In other words, the decrease of the catalyst activity happened faster during the first 24 h, while it declined only 5% in the next 48 hours. Finally, the catalyst activity was reached a constant level that it is understood the catalyst has a_{eq}. S.A. Alsen *et al.* showed that the deactivation of the Fe-K catalyst with monoliths supported at a pressure of 10 atm is performed in two stages of fast and slow. Major changes occur within the first 24 h, and then, at infinite time, the catalyst reaches an equilibrium activity. In addition, according to Fig. 4, the experimental data are in better agreement with Eqs. (5) and (6) (GPLE) than the Eqs. (3) and (4) (PLE). Thus, by using the Eqs. (5)

and (6), the equation of activity rate of the catalyst Fe-K/γ-Al$_2$O$_3$ is obtained as follows;

$$a_{G1} = 0.459 + (1 - 0.459) \times \exp(-0.425 \times t) \tag{9}$$

$$a_{G2} = 0.441 + \left((1.677 \times t) + (\frac{1}{1 - 0.441}) \right)^{-1} \tag{10}$$

a_{G1} is the catalyst activity with the degree of deactivation that is equal to 1, and a_{G2} represents the activity of catalyst with the degree of deactivation equal to 2.

R^2 and R^2_{adj} of both Eqs. (9) and (10) show that the experimental data have matched better with the Eq. (9) due to the amount of variance (Table 2). Therefore, the thorough equation of deactivation rate of catalyst Fe-K/γ Al$_2$O$_3$ is as Eq. (11). In previous studies, GPLE was reported as the best equation for the performance of the iron-based catalyst equation with the degree equal 1.

$$r_d = 0.425 \times (a - 0.459)^1 \tag{11}$$

Investigation of the Effect of Promoter and Support on k_d and a_{eq} in Iron-based Catalyst

In the deactivating equations, it is necessary to obtain the three parameters k_d, a_{eq} and m. If the amounts of k_d and m are high, the catalyst will be deactivated later, and when a_{eq} is large the catalyst will be stable for a longer time. It is
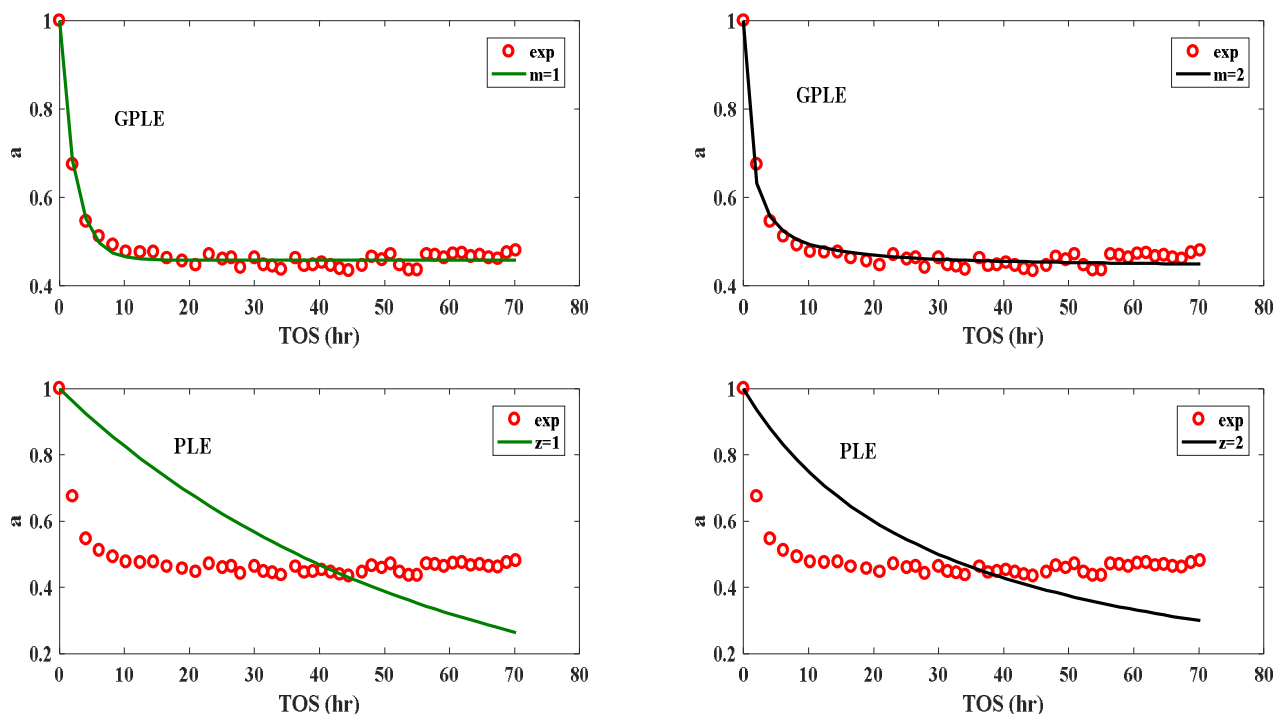
Fig. 4. Matching the experimental data with the values calculated by the equations of GPLE and PLE.

Table 2. Values of Variance, R^2 and R^2_{adj} for the Activity Equations Derived from the GPLE Equation

	R^2	R^2_{adj}	Variance
a_{G1}	0.978	0.977	0.00018
a_{G2}	0.967	0.966	0.00027

obvious that the promoters and supports affect the deactivation rate of the iron-based catalyst. In the following, using the reference data, the effect of Co, Mn promoters and SiO$_2$ support on the k_d, m and a_{eq} is investigated. Then, utilizing the reference data 29 and the data achieved in this study, the effect of temperature on the deactivating rate parameters (k_d, m, a_{eq}) will be also studied.

According to Table 3, the presence of potassium in the Fe/Cu/Al catalyst does not modify the deactivation rate degree (m), and for both Fe/Cu/Al and Fe/Cu/K/Al catalysts, m = 2 is suitable. However, the presence of K

leads to a 76% loss in the deactivation rate constant and a 15.6% increase of a_{eq} of the Fe/Cu/Al catalytic.

Under the same operating conditions, the Fe/K catalyst in the vicinity of Al$_2$O$_3$ and SiO$_2$ supports has m = 1, and for this catalyst, k_d and a_{eq} are respectively reduced to 97% and 52% with the alumina support, compared to the silicate support.

Comparing the fifth row with the third and fourth rows in Table 3, it is understood that when the catalyst Fe/K is employed without the support, the deactivation rate degree, m, shifts from 1 to 2. And when the manganese promoter is

Table 3. The Parameters of Deactivation Rate Obtained for a Variety of Iron-based Catalysts

	Catalyst	Temperature (°C)	Pressure (MPa)	Order one (m = 1)				Order tow (m = 2)			
				k_d	a_{eq}	R^2	R^2_{adj}	k_d	a_{eq}	R^2	R^2_{adj}
1	Fe/Cu/Al [28]	300	1.01	0.02	0.678	0.99	0.988	0.030	0.515	0.99	0.99
2	Fe/K/Cu/Al [28]	300	1.01	0.003	0.600	0.971	0.97	0.007	0.61	0.97	0.97
3	Fe/K/Al$_2$O$_3$ [29]	250	1.5	0.001	0.429	0.91	0.906	0.0036	0.505	0.908	0.90
4	Fe/K/SiO$_2$ [29]	250	1.5	0.051	0.896	0.977	0.976	0.31	0.86	0.96	0.96
5	Fe/K [30]	250	1.5	0.05	0.890	0.79	0.77	0.34	0.85	0.80	0.79
6	Fe/K/Mn [30]	250	1.5	0.03	0.920	0.934	0.93	0.24	0.89	0.943	0.937
7	Fe-K/Al$_2$O$_3$ (in this paper)	310	0.2	0.43	0.460	0.978	0.977	1.677	0.44	0.967	0.966
8	Fe/K/Mn/Al$_2$O$_3$ [31]	300	0.3	0.113	0.841	0.95	0.95	0.65	0.81	0.96	0.96
9	Fe/Mn/Al$_2$O$_3$[32]	220	0.6	0.105	0.789	0.994	0.994	0.805	0.82	0.96	0.96

added to it, the amount of k_d decreases 29% and normal balanced activity increases 4%.

The manganese promoter enhances reduction of the iron-based catalyst in the atmosphere of hydrogen, while the power of basic sites is reduced by the interactions between potassium and manganese. The degree of deactivation rate changes from 1 to 2 and k_d and a_{eq} also increases, respectively 34% and 43% with the presence of manganese in the catalyst Fe/K on the alumina support.

As a result of the presence of the manganese promoter in the catalyst Fe/Al$_2$O$_3$, a_{eq} reaches 78.9% of its initial value after about 70 h while the potassium decreases a_{eq} of the catalyst Fe/Al$_2$O$_3$ to 54% in the same period.

In this study, the rate of deactivation of the Fe-K/Al$_2$O$_3$ catalyst at temperatures 250 and 310 °C and pressures of 0.2 MPa to 1.5 MPa is equal to one, but with a decrease in the temperature to 60 °C, the amount of k_d lessens to 99.7%, in the case that the balance normal activity has the little changes in 70 h.

CONCLUSIONS

Deactivation of the catalyst over time is the most important challenge of catalytic processes in the industry. In the Fischer-Tropsch process, a variety of products and the intermediate of materials are made. In addition, significant amounts of water, carbon sediment, and CO$_2$ are produced, which can significantly affect the catalyst deactivation. Most importantly, the FT reaction is highly exothermic, which can cause catalyst sintering by creating the hot site. The use of deactivation models is not so expensive as laboratory scales and simulation projects. The effect of effective parameters on the catalyst activity, including changes in reaction conditions, the presence or absence of the promoter, and also the effect of support can be expressed quantitatively through these models. For the Fe/K/Al$_2$O$_3$ catalyst, the deactivation rate equation was obtained with the deactivation degree of one and so k_d and the normal activity are 0.425 and 0.459, respectively. It was

also found that the effect of the potassium promoter in iron-based catalyst has no effect on the deactivation rate degree but reduces k_d significantly. The presence of alumina-support on the Fe/K catalyst caused a decrease in the degree of deactivation rate and a_{eq}. The manganese promoter in the iron-based catalyst raises the selectivity of heavy hydrocarbons, and also improves the reduction of this catalyst, however it adds the degree of deactivation rate and thus increases the rate of deactivation of Fe/K catalyst.

ACKNOWLEDGEMENTS

LIST OF SYMBOLS

a	Normalized activity
a_{eq}	Normal balanced activity
a_G	Activity taking into account the normal activity at infinite time
a_{G1}	Activity taking into account the normal activity at infinite time, m = 1
a_{G2}	Activity taking into account the normal activity at infinite time, m = 2
a_p	Activity without account the normal activity at infinite time
C_{in}	Concentration input
C_{out}	Concentration output
k_d	Constant values of deactivation rate
k'_d	Deactivation rate constant taking into account the normal activity at infinite time
m	The degree of deactivation for r_{dG}
R^2	Correlation coefficient
R^2_{adj}	Adjusted coefficient
r_d	The rate of catalyst deactivation
r_{dG}	The rate of catalyst deactivation taking into account the normal activity at infinite time
r_{dP}	The rate of catalyst deactivation without account the normal activity at infinite time
t	Time (s)
X	Conversion
z	The degree of deactivation for r_{dP}

REFERENCES

[1] Comazzi, A.; Pirola, C.; Longhi, M.; Bianchi, C. L. M.; Suslick, K. S., Fe-based heterogeneous catalysts for the Fischer-Tropsch reaction: Sonochemical synthesis and bench-scale experimental tests. *Ultrason. Sonochem.* **2017**, *34*, 774-780, DOI: 10.1016/j.ultsonch.2016.07.012.

[2] Selvatico, D.; Lanzini, A.; Santarelli, M., Low temperature Fischer-Tropsch fuels from syngas: kinetic modeling and process simulation of different plant configurations. *Fuel* **2016**, *186*, 544-560, DOI: 10.1016/j.fuel.2016.08.093.

[3] Tijmensen, M. J. A.; Faaij, A. P. C.; Hamelinck, C. N.; Van Hardeveld, M. R. M., Exploration of the possibilities for production of Fischer Tropsch liquids and power via biomass gasification. *Biomass and Bioenergy* **2002**, *23*, 129-152, DOI: 10.1016/S0961-9534(02)00037-5.

[4] Razmjooie, A.; Atashi, H.; Shahraki, F., The application of hybrid RSM/ANN methodology of an iron-based catalyst performance in Fischer-Tropsch synthesis. *Phys. Chem. Res.* **2017**, *5*, 585-600, DOI: 10.22036/PCR.2017.72773.1346.

[5] Mirzaei, A. A.; Arsalanfar, M.; Bozorgzadeh, H. R.; Samimi, A., A review of Fischer-Tropsch synthesis on the cobalt based catalysts, *Phys. Chem. Res.* **2014**, *2*, 179-201, DOI:10.22036/PCR.2014.5786.

[6] Mirzaei, A. A.; Golestan, S.; Barakati, S. -M., prediction of Fe-Co-Mn/MgO catalytic activity in Fischer-Tropsch synthesis using nu-support vector regression, *Phys. Chem. Res.* **2016**, *4*, 391-405, DOI: 10.22036/PCR.2016.14776.

[7] Farsad, M.; Elahifard, M.; Behjatmanesh-Ardakani, R., The effect of Cu impurity on the CO-dissociation mechanism on the Fe (100) surface: A full potential DFT study, *Phys. Chem. Res.* **2017**, *5*, 831-839, DOI: 10.22036/pcr.2017.90235.1392.

[8] Abelló, S.; Montané, D., Exploring iron-based multifunctional catalysts for fischer-tropsch synthesis: A review, *Chem. Sus. Chem.* **2011**, *4*, 1538-1556, DOI: 10.1002/cssc.201100189.

[9] Mirzaei, A. A.; Arsalanfar, M.; Ebrahimzadeh, F.; Atashi, H.; Mirhoseini Moghaddam, S. H., Kinetic study of Fischer Tropsch synthesis over co precipitated iron-cerium catalyst, *Phys. Chem. Res.* **2013**, *1*, 69-80, DOI: 10.22036/PCR.2013.2641.

[10] Khodakov, A. Y.; Chu, W.; Fongarland, P., Advances in the development of novel cobalt Fischer-Tropsch catalysts for synthesis of long-chain hydrocarbons and clean fuels, *Chem. Rev.* **2007**, *107*, 1692-1744, DOI: 10.1021/cr050972v.

[11] Hu, J.; Yu, F.; Lu, Y., Application of Fischer-Tropsch synthesis in biomass to liquid conversion, catalysts **2012**, 2, 303-326, DOI: 10.3390/catal2020303.

[12] Bartholomew, C. H., Mechanisms of catalyst deactivation, *Appl. Catal. A Gen.* **2001**, *212*, 17-60, DOI: 10.1016/S0926-860X(00)00843-7.

[13] Tsakoumis, N. E.; Rønning, M.; Borg, Ø.; Rytter, E.; Holmen, A., Deactivation of cobalt based Fischer-Tropsch catalysts: A review, *Catal. Today* **2010**, *154*, 162-182, DOI: 10.1016/j.cattod.2010.02.077.

[14] De Smit, E.; Weckhuysen, B. M., The renaissance of iron-based Fischer-Tropsch synthesis: on the multifaceted catalyst deactivation behaviour, *Chem. Soc. Rev.* **2008**, *37*, 2758, DOI: 10.1039/b805427d.

[15] Hwang, J. S.; Jun, K. W.; Lee, K. W., Deactivation and regeneration of Fe-K/alumina catalyst in CO2hydrogenation, *Appl. Catal. A Gen.* **2001**, *208*, 217-222, DOI: 10.1016/S0926-860X(00)00701-8.

[16] Argyle, M.; Bartholomew, C., Heterogeneous catalyst deactivation and regeneration: A review, *Catalysts* **2015**, *5*, 145–269, DOI: 10.3390/catal5010145.

[17] Ngantsoue-Hoc, W.; Zhang, Y.; Brien, R. J.; Luo, M.; Davis, B. H., Fischer-Tropsch synthesis: Activity and selectivity for Group I alkali promoted iron-based catalysts, *Appl. Catal. A Gen.* **2002**, *236*, 77-89, DOI: 10.1016/S0926-860X(02)00278-8.

[18] Bui, L. H.; De Klerk, A., Thermal behavior of potassium C1-C12 n -alkanoates and its relevance to fischer-tropsch, *J. Chem. Eng. Data* **2014**, *59*, 400-411, DOI: 10.1021/je400874d.

[19] Yang, Y.; Xiang, H. -W.; Xu, Y. -Y.; Bai, L.; Li, Y. -W., Effect of potassium promoter on precipitated

iron-manganese catalyst for Fischer-Tropsch synthesis, *Appl. Catal. A Gen.* **2004**, *266*, 181-194, DOI: 10.1016/j.apcata.2004.02.018.

[20] Ding, F.; Zhang, A.; Liu, M.; Zuo, Y.; Li, K.; Guo, X.; Song, C., CO2 hydrogenation to hydrocarbons over iron-based catalyst: Effects of physicochemical properties of Al2O3 supports, *Ind. Eng. Chem. Res.* **2014**, *53*, 17563-17569, DOI: 10.1021/ie5031166.

[21] Jun, K. W.; Lee, S. J.; Choi, M. J.; Lee, K. W., Catalytic hydrogenation of CO2 into hydrocarbons: Support effects on Fe and Fe-K catalysts, *ACS Div. Fuel Chem. Prepr.* **1996**, *41*, 1411-1413.

[22] Cubeiro, M. L.; Morales, H.; Goldwasser, M. R.; Perez-Zurita, M. J.; Gonzalez-Jimenez, F.; Urbina de N, C., Hydrogenation of carbon oxides over Fe/Al2O3 catalysts, *Appl. Catal.* **1999**, *189*, 87-97, DOI: 10.1016/S0926-860X(99)00262-8.

[23] Lee, S. C.; Jang, J. H.; Lee, B. Y.; Kang, M. C.; Kang, M.; Choung, S. J., The effect of binders on structure and chemical properties of Fe-K/γ-Al2O3 catalysts for CO2 hydrogenation, *Appl. Catal. A Gen.* **2003**, *253*, 293-304, DOI: 10.1016/S0926-860X(03)00540-4.

[24] Eliason, S. A.; Bartholomew, C. H., Kinetics and deactivation of unpromoted and potassium-promoted iron fischer-tropsch catalysts at low pressure (1 Atm), *Stud. Surf. Sci. Catal.* **1991**, *68*, 211-218, DOI: 10.1016/S0167-2991(08)62635-X.

[25] Eliason, S. A.; Bartholomew, C. H., Reaction and deactivation kinetics for Fischer–Tropsch synthesis on unpromoted and potassium-promoted iron catalysts, *Appl. Catal. A Gen.* **1999**, *186*, 229-243, DOI: 10.1016/S0926-860X(99)00146-5.

[26] Hong, J. S.; Hwang, J. S.; Jun, K. W.; Sur, J. C.; Lee, K. W., Deactivation study on a coprecipitated Fe-Cu-K-Al catalyst in CO2 hydrogenation, *Appl. Catal. A Gen.* **2001**, *218*, 53-59, DOI: 10.1016/S0926-860X(01)00617-2.

[27] Bartholomew, C. H., Sintering kinetics of supported metals: new perspectives from a unifying GPLE treatment, *Appl. Catal. A, Gen.* **1993**, *107*, 1-57, DOI: 10.1016/0926-860X(93)85114-5.

[28] Jun, K. W.; Roh, H. S.; Kim, K. S.; Ryu, J. S.; Lee, K. W., Catalytic investigation for Fischer-Tropsch

synthesis from bio-mass derived syngas, *Appl. Catal. A Gen.* **2004**, *259*, 221-226, DOI: 10.1016/ j.apcata.2003.09.034.

[29] Zhao, G.; Zhang, C.; Qin, S.; Xiang, H.; Li, Y., Effect of interaction between potassium and structural promoters on Fischer-Tropsch performance in iron-based catalysts, *J. Mol. Catal. A Chem.* **2008**, *286*, 137-142, DOI: 10.1016/ j.molcata.2008.02.019.

[30] Tao, Z.; Yang, Y.; Wan, H.; Li, T.; An, X.; Xiang, H.; Li, Y., Effect of manganese on a potassium-promoted iron-based Fischer-Tropsch synthesis catalyst, *Catal. Lett.* **2007**, *114*, 161-168, DOI:

10.1007/s10562-007-9060-6.

[31] Fazlollahi, F.; Sarkari, M.; Gharebaghi, H.; Atashi, H.; Zarei, M. M.; Mirzaei, A. A.; Hecker, W. C., Preparation of Fe-Mn/K/Al₂O₃ Fischer-Tropsch catalyst and its catalytic kinetics for the hydrogenation of carbon monoxide, *Chinese J. Chem. Eng.* **2013**, *21*, 507-519, DOI:10.1016/S1004-9541(13)60503-0.

[32] Sarkari, M.; Fazlollahi, F.; Atashi, H.; Mirzaei, A. A.; Hecker, W. C., Using different preparation methods to enhance fischer-tropsch products over iron-based catalyst, *Chem. Biochem. Eng. Q.* **2013**, *27*, 259-266.